# A new type V toxin-antitoxin system where mRNA for toxin GhoT is cleaved by antitoxin GhoS

Xiaoxue Wang[1,2,9], Dana M Lord[3,9], Hsin-Yao Cheng[4,9], Devon O Osbourne[4], Seok Hoon Hong[2], Viviana Sanchez-Torres[2], Cecilia Quiroga[4], Kevin Zheng[5], Torsten Herrmann[6], Wolfgang Peti[3], Michael J Benedik[7], Rebecca Page[5]* & Thomas K Wood[2,4,7,8]*

**Among bacterial toxin-antitoxin systems, to date no antitoxin has been identified that functions by cleaving toxin mRNA. Here we show that YjdO (renamed GhoT) is a membrane lytic peptide that causes ghost cell formation (lysed cells with damaged membranes) and increases persistence (persister cells are tolerant to antibiotics without undergoing genetic change). GhoT is part of a new toxin-antitoxin system with YjdK (renamed GhoS) because *in vitro* RNA degradation studies, quantitative real-time reverse-transcription PCR and whole-transcriptome studies revealed that GhoS masks GhoT toxicity by cleaving specifically *yjdO* (*ghoT*) mRNA. Alanine substitutions showed that Arg28 is important for GhoS activity, and RNA sequencing indicated that the GhoS cleavage site is rich in U and A. The NMR structure of GhoS indicates it is related to the CRISPR-associated-2 RNase, and GhoS is a monomer. Hence, GhoT-GhoS is to our knowledge the first type V toxin-antitoxin system where a protein antitoxin inhibits the toxin by cleaving specifically its mRNA.**

Toxin-antitoxin systems are found in nearly all bacterial chromosomes[1], which attests to their importance in cell physiology. Toxin-antitoxin systems are classified as type I if the antitoxin RNA prevents the translation of toxin RNA, type II if the antitoxin protein binds and inhibits the toxin protein and type III if the antitoxin RNA binds and inhibits the protein toxin[2]. Also, a type IV designation has been proposed recently for a toxin-antitoxin system in which the protein antitoxin interferes with binding of the toxin to its target rather than inhibits the toxin via direct toxin-antitoxin binding[3]. Toxins inhibit growth (for example, inhibit translation via mRNA degradation), and antitoxins reduce toxin activity; however, antitoxins are generally labile under various stress conditions, which results in toxin activation[2].

The role of toxin-antitoxin systems in cell physiology, specifically in biofilm formation[4,5], persister cell formation[6,7] and the general stress response[8,9], is becoming more clear. Notably, mRNA endoRNase toxins are becoming recognized as global regulators that alter gene regulation by cleaving specific mRNAs (termed differential mRNA decay)[10]. For example, upon antibiotic stress, toxin MazF degrades most mRNAs with ACA sequences. However, its activity also results in the preferential synthesis of a subset of small proteins whose mRNAs are not degraded[11]. As these enriched proteins are necessary both for toxicity and for survival[11], MazF acts as a regulatory factor[12].

The toxin motility quorum sensing regulator (MqsR, YgiU/B3022)[4,13] is also a global regulator[13,14] and is conserved in 40 eubacteria[13]. Its specific mRNA endoRNase activity leads to enrichment of mRNAs that code for the stress-associated proteins CstA, CspD, RpoS, Dps and HokD[14]. In addition, 14 *Escherichia coli* mRNA transcripts do not contain the MqsR-preferred GCU cleavage site[15,16],

and 6 of these (*pheL*, *tnaC*, *trpL*, *yciG*, *ygaQ* and *ralR*) are differentially regulated in biofilms[17]. Another one of these 14 transcripts that lacks GCU sites is *yjdO* (B4559, renamed here as *ghoT* for 'toxin-producing ghost cells'); the protein it encodes is conserved in *E. coli* and *Shigella* spp. and has not been previously characterized.

As an indicator of its impact on cell physiology through differential mRNA decay, MqsR is the first toxin that, upon inactivation, decreases the formation of persister cells[6]. Persister cells are a small fraction of bacteria that show tolerance to antibiotics without genetic change[18]; it is believed that they survive antibiotic treatment by becoming metabolically dormant[19]. The crucial regulator of MqsR toxicity, antitoxin MqsA (YgiT/B3021)[20], is the first antitoxin shown to be a global regulator, as transcription of loci such as *rpoS* are derepressed upon MqsA degradation during oxidative stress[9,14] and have critical roles in bacterial cell physiology during stress.

It is well established that endoRNase toxins, including MqsR[6] and RelE[21], and the kinase HipA[21,22] inhibit protein synthesis, which is correlated with the formation of persister cells and, in turn, an increase in multidrug tolerance. Moreover, isolated persister cells also show increased transcription of the toxin genes *mqsR*[23], *relE*[21] and *mazF*[21]. The mechanism (or mechanisms) underlying the increased persistence observed upon expression of these toxins, however, has not been fully characterized. Here we present evidence that the product of one of the transcripts that lacks the primary MqsR GCU site, GhoT, increases persistence and that GhoT-GhoS (YjdO-YjdK) is a new toxin-antitoxin system. We show that toxin GhoT, when produced, leads to both cell death and, in the absence of cell death, an increase in persister cells. Moreover, GhoT-GhoS is to our knowledge the first non–type I chromosomal toxin-antitoxin system that encodes a presumed membrane-lytic protein.

Unexpectedly and most interestingly, the antitoxin GhoS does not function like a typical antitoxin, as it is not labile during stress and does not bind DNA to regulate transcription. Because its sequence does not resemble any protein whose structure or function is known, we used biomolecular NMR spectroscopy to determine its three-dimensional structure. GhoS adopts a ferredoxin-like fold that is most similar to that of CRISPR-associated-2 (CAS2) sequence-specific endoRNases. We show that GhoS is a sequence-specific endoRNase that cleaves *ghoT* mRNA, preventing its translation. Thus, GhoT-GhoS is to our knowledge the first example of a toxin-antitoxin system where the antitoxin protein cleaves the toxin mRNA; we classify this as a type V toxin-antitoxin system.

## RESULTS
### GhoT increases persistence

Initially, we examined the 14 *E. coli* transcripts that lack GCU sites to determine whether they were related to the ability of MqsR to increase persistence[6]. We investigated the effect of producing MqsR from pCA24N-*mqsR* in each of the 14 isogenic single-gene knockouts (*ghoT, hisL, kilR, pheL, ralR, tnaC, trpL, yahH, ybfQ, ybhT, yciG, ygaQ, yheV* and *ymdF*) (**Supplementary Results**, **Supplementary Table 1**) 2 h after the addition of ampicillin (100 μg ml⁻¹) to determine whether the ability of MqsR to increase persistence was altered and found that deleting *ghoT* had one of the greatest effects on MqsR-mediated persistence (**Supplementary Table 2**). In strains where the kanamycin gene replacement might create a polar effect, we removed the resistance gene and retested the strains. In no case could the effects be ascribed to polarity (**Supplementary Table 2**). A time-course study further confirmed that deleting *ghoT* significantly ($P < 0.05$) reduced MqsR-mediated persistence ($27 \pm 2$-fold reduction) for Δ*ghoT*/pCA24N-*mqsR* versus BW25113/pCA24N-*mqsR*) and made the cell behave similarly to the wild-type strain without MqsR production (**Fig. 1a**). Corroborating the dependence of MqsR on GhoT to increase persistence, producing GhoT in a Δ*ghoT* strain also increased persistence $48 \pm 3$-fold to levels seen when MqsR was produced (**Fig. 1b**). In fresh LB medium, some of these persister cells revived with a lag time of roughly 4 h, which is comparable to reported values[24] (**Fig. 1c**).

### GhoT affects the membrane and produces ghost cells

The organization of the *ghoST* operon and the impact of GhoT on persistence suggested that GhoS and GhoT might be a toxin-antitoxin pair (**Supplementary Fig. 1a**). Hence, we tested whether or not GhoT is a toxin. GhoT is predicted to be a small (57 residues), highly hydrophobic protein with two transmembrane domains (residues 7–27 and 37–57)[25]. When GhoT was produced in the wild-type strain, which contains a chromosomal gene for the putative antitoxin GhoS, the turbidity of the culture decreased (**Fig. 2a**), and this decrease was due to cell lysis as cell cultures became clear (**Fig. 2b**). Corroborating these results, production of GhoT caused 60% of the

cells to adopt 'ghost' morphologies as observed using phase contrast microscopy (**Fig. 2c**); ghost cells are dead or dying cells in which the damaged membrane causes the cell poles to appear dense and the center to appear transparent[26]. Therefore, GhoT is a toxin that, when overproduced, lyses cells by disrupting the cell membrane to form ghost cells.

### GhoT and GhoS form a toxin-antitoxin pair

Like toxin GhoT, GhoS is also a small protein (98 residues). There are 27 base pairs (bp) between the two genes, which include a putative RBS for *ghoT*; therefore, *ghoS* and *ghoT* are predicted to comprise a single operon, *ghoST*. Unlike production of GhoT, production of GhoS was not toxic, and it completely counteracted the toxicity of GhoT (**Fig. 2a**). Furthermore, production of GhoS with GhoT reduced the formation of ghost cells by a factor of 18, as shown through microscopic observation of ~500 cells (**Fig. 2c**), whereas producing GhoS alone did not cause ghost cells to form.

Replacement of antitoxin *ghoS* with a kanamycin cassette[27] is not lethal, which is most likely a result of the polar effect on downstream *ghoT*. However, when GhoT was produced via pCA24N-*ghoT*, deletion of *ghoS* was lethal as growth was completely inhibited in the Δ*ghoS* mutant but not in the Δ*ghoT* mutant, which has an intact chromosomal copy of *ghoS* (**Fig. 2d**). This growth inhibition from toxin production in the absence of the antitoxin is a typical feature of toxin-antitoxin systems[20], although polar mutations can mask this effect if the antitoxin gene precedes the toxin gene.

As shown by PCR with reverse transcription (RT-PCR), *ghoST* form a single operon as they are transcribed together. Specifically, we detected a single band of ~400 bp using a forward primer in the first gene (*ghoS*-f) and a reverse primer in the second gene (*ghoT*-r) (**Supplementary Table 3**) using cDNA synthesized from total RNA as the template (**Supplementary Fig. 1b**). As a control, we detected the same band using genomic DNA as a template, but this band was not seen using total RNA as a template. Collectively, these results demonstrate that GhoS is an antitoxin, that *ghoT* and *ghoS* are transcribed together and that they form a toxin-antitoxin system.

### GhoS is a proteic monomeric antitoxin

To demonstrate that GhoS functions as a proteic antitoxin, we introduced a stop codon by a single nucleotide change in *ghoS* DNA encoding Tyr16 and tested its impact on cell growth. We found that the early termination mutation abolished the ability of GhoS to block the toxicity of GhoT for both cell growth (**Fig. 2a**) and ghost cell formation. We also found that antitoxin GhoS is not degraded (**Supplementary Fig. 2a**) in response to stress[28], whereas most antitoxins are degraded (**Supplementary Fig. 2b**), and found that GhoS does not bind its own promoter (**Supplementary Fig. 3**). In addition, size-exclusion chromatography, dynamic light scattering (**Supplementary Fig. 4**) and biomolecular NMR experiments
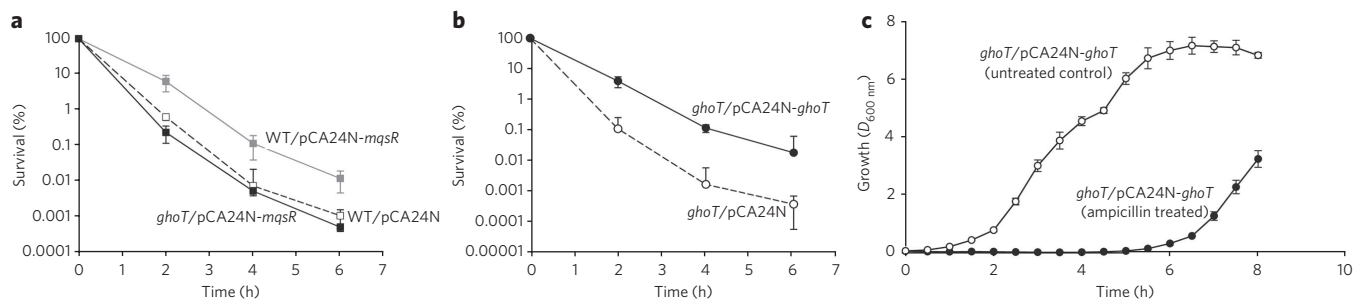


**Figure 1 | GhoT increases persistence.** (**a,b**) Cell survival after ampicillin (100 μg ml⁻¹) treatment for 2 h, 4 h and 6 h with MqsR production with and without *ghoT* (**a**) or with GhoT production (**b**). WT, wild-type host (*E. coli* BW25113). (**c**) Revival of GhoT-induced persister cells was tested by producing GhoT in BW25113 *ghoT*/pCA24N-*ghoT* while treating cells with ampicillin (100 μg ml⁻¹) for 2 h. Growth in fresh LB medium was compared to control cells that lacked ampicillin treatment. At least three independent cultures of each strain were evaluated for each experiment. Error bars, ± s.e.m.

(described below) demonstrated that GhoS is a monomer in solution. Collectively, these results show that GhoS is a noncanonical antitoxin because it does not regulate its own transcription, is stable and is a monomer in solution.
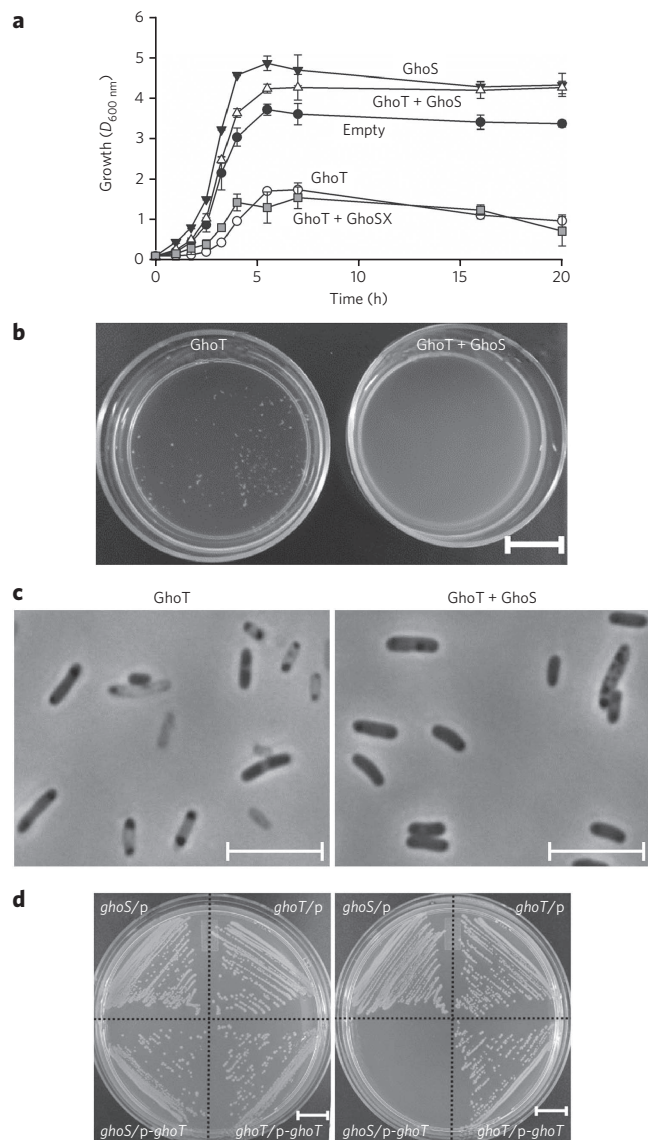
**Figure 2 | GhoT is toxic, and GhoS reduces this toxicity.** (**a**) Cell growth in LB medium for cells producing GhoT and GhoS. The chromosomal copy of *ghoS* in the wild-type strain allows for some growth with toxin GhoT production. GhoSX is truncated GhoS with a stop codon introduced at Tyr16. Three independent cultures of each strain were evaluated. Error bars, ± s.e.m. (*n* = 3). (**b**) Cell culture at the end of growth in **a** at 20 h to show the clearance and lysis due to production of GhoT. Scale bars, 1 cm. (**c**) Cell morphology after incubating for 8 h at 37 °C. Scale bars, 5 μm. For **a–c**: Empty, BW25113/pCA24N/pBS(Kan); GhoT, BW25113/pCA24N-*ghoT*/pBS(Kan); GhoS, BW25113/pCA24N/pBS(Kan)-*ghoS*; GhoT + GhoS, BW25113/pCA24N-*ghoT*/pBS(Kan)-*ghoS*; GhoT + GhoSX, BW25113/pCA24N-*ghoT*/pBS(Kan)-*ghoS*X. Plasmids were retained with kanamycin (50 μg ml⁻¹) and chloramphenicol (30 μg ml⁻¹); 0.5 mM IPTG was used at time 0 to produce the plasmid-based proteins. Three independent cultures of each strain were evaluated. (**d**) Growth on LB plates with kanamycin (50 μg ml⁻¹) and chloramphenicol (30 μg ml⁻¹) without (left) or with (right) IPTG (1 mM, to induce *ghoT* via pCA24N-*ghoT*). In the absence of a chromosomal copy of *ghoS*, there is no growth with toxin GhoT production. *ghoS*, BW25113 Δ*ghoS*; *ghoT*, BW25113 Δ*ghoT*; p, pCA24N; p-*ghoT*, pCA24N-*ghoT*. Three independent cultures of each strain were evaluated. Scale bars, 1 cm.

## GhoS adopts a ferredoxin-like fold similar to CAS2

Analysis of the GhoS protein sequence using BLAST revealed that although it is conserved among multiple species of *E. coli*, it is not similar to any protein whose structure or function is known. Because function is more highly conserved than sequence, we used biomolecular NMR spectroscopy to determine the structure of GhoS and, in turn, gain insights into its biological function. In the sequence-specific backbone assignment, 95 of the expected 96 backbone amide NH pairs (three prolines) are assigned, with the missing residue corresponding to the N-terminal cloning artifact His(−1) (**Supplementary Fig. 5**). A total of 2,479 NOE-derived distance constraints were used for the structure calculation (~25 NOE constraints per residue) using a simulated annealing protocol within the program CYANA[29–31] and refined in explicit solvent using the program CNS[32]. The GhoS model has excellent stereochemistry (**Supplementary Methods**), and the r.m.s. deviation about the mean coordinate positions of the backbone atoms for residues 5–95 is 0.36 ± 0.08 Å (20 models in the ensemble; **Supplementary Fig. 6a**). NMR and refinement statistics are reported in **Supplementary Table 4**. The three-dimensional GhoS structure consists of three α-helices and five β-strands (**Fig. 3a**) and is stabilized by two hydrophobic clusters. The central hydrophobic core consists of residues Tyr10, Val12, Phe14, Tyr16, Phe24, Leu27, Met31, Met34, Phe36, Phe55, Ile57, Ile66, Ile70, Leu77, Ile80, Phe82, Leu84 and Ile86 (**Supplementary Fig. 6b**). The structure is also stabilized by a second hydrophobic cluster comprising Val11, Val40, Leu50, Ala56, Met87, Val89, Tyr92 and Phe93 (**Supplementary Fig. 6c**).

A search for structural homologs of GhoS using the structure-based alignment program DALI[33] identified six proteins with *Z* scores of 5.8 to 6.3, all of which adopt a ferredoxin-like fold, characterized by a split α-β sandwich (β-α-β-β-α-β; **Supplementary Table 5**). This superfold is highly populated with functionally diverse proteins, such as ribosomal proteins, DNA binding proteins and RNases[34]. Of the six structures with the best *Z* scores, only two were of similar size to GhoS: SSO1404 (Protein Data Bank (PDB) code 2I8E, 88 residues; *Z* score = 6.1)[35] and SSO8090 (PDB code 3EXC, 78 residues; *Z* score = 5.8). These proteins (and three other family members: TT1823, *Z* score = 5.6; PF1117, *Z* score = 5.1; DvuCAS2, *Z* score = 5.0 (ref. 36)) belong to the CAS2 family. SSO1404 and SSO8090 are sequence-specific endoRNases that preferentially cleave single-stranded RNA[37]. The structures of GhoS and the CAS2 protein SSO1404 monomer (CAS2 proteins are dimers *in vitro*) overlap well (**Supplementary Figs. 6d,e** and **7**). The primary difference between them is the position of β-strand β2. In GhoS, β2 and β2′ form a short two-stranded β-sheet that interacts with the C-terminal α-helix, α3. In contrast, in the CAS2 proteins, β2 projects upwards to form the fourth β-strand of the β-sheet in the ferredoxin fold. Thus, GhoS adopts an atypical ferredoxin fold in which the central β-sheet is made up of three and not four β-strands.

## GhoS is an endoRNase that cleaves *ghoT* mRNA

The sequence identity between GhoS and the CAS2 proteins is low (10–19%). However, when the structures of SSO1404 and GhoS are superimposed, five of the six SSO1404 catalytic residues are structurally conserved in GhoS (**Fig. 3a** and **Supplementary Fig. 6d,e**; GhoS-SSO1404 conserved residues: Phe14-Tyr9, Asp15-Asp10, Arg26-Arg19, Arg28-Arg31 and Phe55-Phe37). Systematically converting these five GhoS residues to alanines revealed that, *in vitro*, the R28A, F55A and, to a lesser extent, R26A substitutions reduced the ability of antitoxin GhoS to cleave *ghoT* mRNA (**Fig. 3b** and **Supplementary Fig. 8**; CD shows all mutants are folded in **Fig. 3c**); this effect was also corroborated for the R28A variant *in vivo* (**Fig. 3d**). Thus, Arg28 seems to be important for GhoS activity.

Because GhoS production is not toxic but instead increases growth (**Fig. 2a**), these results suggest that GhoS is a sequence-specific endoRNase. Thus, we investigated whether GhoS cleaves
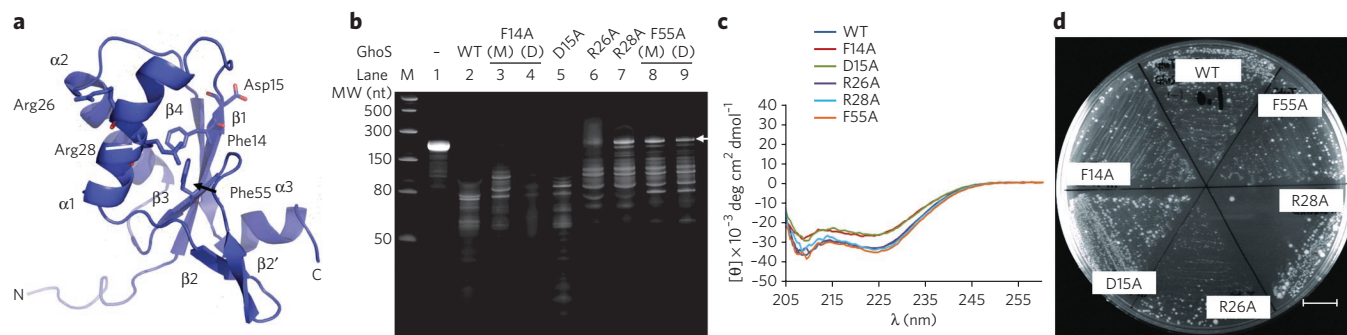
**Figure 3 | GhoS adopts a ferredoxin-like fold and Arg28 is important for its cleavage activity.** (**a**) Ribbon model of the lowest-energy conformer of GhoS, with the secondary structural elements and termini labeled; putative catalytically important residues shown as sticks and labeled. Figure prepared with PyMOL (http://www.pymol.org/). (**b**) Two micrograms of in vitro synthesized wild-type *ghoT* transcript (207 nt, lane 1) were incubated without (−) or with 30 µg of purified GhoS and its variants at 37 °C for 3 h. Two mutants, F14A and F55A, were eluted from the size-exclusion column as monomers (M) and dimers (D), so both forms were tested (F14A, 40% dimer; F55A, 32% dimer). The reduced activity of GhoS with point mutations is shown by the presence of uncleaved transcript, as indicated by an arrow. MW, low-range single-stranded RNA ladder with lengths indicated in nt; WT, wild type. (**c**) CD spectra demonstrating that native GhoS (dark blue) and all of the GhoS mutants are folded (sample concentrations ~20 µM). (**d**) Coexpression of GhoT with wild-type (WT) GhoS and the GhoS variants via BL21(DE3)/pCA24N-*ghoT* harboring the pRP1B(Kan)-*ghoS* constructs (0.1 mM IPTG was used). Scale bar, 1.1 cm.

*ghoT* mRNA. Using quantitative real-time reverse-transcription PCR (qRT-PCR), we found that the *ghoT* portion of the *ghoST* transcript in the wild-type strain was $21 \pm 2$-fold less stable than the *ghoS* portion of the transcript in the stationary phase (all qRT-PCR data is in **Supplementary Table 6**). Corroborating this result, production of GhoS via pCA24N-*ghoS* reduced the *ghoT* portion of the transcript $5 \pm 1$-fold relative to the empty plasmid. Cleavage by GhoS seems specific because GhoS production had little effect on the transcript level of *ompA*, *ompF*, *ralR* and *purA* relative to the effects of the empty plasmid (fold changes of $-1.1 \pm 0.2$, $1.2 \pm 0.1$, $-1.7 \pm 0.4$ and $-1.9 \pm 0.5$, respectively).

*In vitro*, GhoS cleaved the *ghoT* portion of the transcript (207 nucleotides (nt), **Supplementary Table 7**) at multiple sites and generated, after full digestion, fragments of approximately 52 nt, 65 nt, 87 nt, 91 nt and 116 nt (**Fig. 4a** and **Supplementary Fig. 8**), whereas there was less degradation of the *ghoS* portion of the transcript under the same conditions. As expected, heat denaturation of GhoS abolished the ability to cleave the transcripts. We observed very little degradation of the ATP synthase subunit gene *atpE* and *ompA* in vitro. Finally, we observed no degradation of: (i) total RNAs *in vitro*, (ii) 23S and 16S rRNAs *in vivo* with GhoS and (iii) tRNAs *in vitro* (**Supplementary Fig. 9**).

Using RNA sequencing, we found that GhoS cleaves specifically *ghoT* mRNA between nt positions 30-31, 51-52, 66–68, 115-116 and 154-155 (positions S1 to S5, respectively; **Fig. 4b**). Analysis of the cleaved products identified a putative cleavage site corresponding to 5′-UNNU(A/C)N(A/G)(A/U)A(A/U)-3′ (where N is A, C, G or T). To corroborate GhoS cleavage at the 51-52 nt site, we altered the *ghoT* mRNA fragment via mutation m1 (AUAUU to CGCGC at nt 52–56; **Fig. 4b**) and found a reduction in overall cleavage and an increase in larger fragments (for example, 87 nt and 124 nt), as would be expected for loss of this site (**Fig. 4c**). Additional mutations (m2 at nt 125–128 and m3 at nt 59–64) reduced cleavage as expected given their proximity to cleavage sites 66–68 and 115-116, and the m4 change (at nt 132–137, not near a cleavage site) had little effect because the transcript was completely degraded, as with the wild-type *ghoT* mRNA (**Fig. 4c**).

To investigate the importance of RNA secondary structure on GhoS cleavage, we recovered the stems in secondary structure disrupted by mutations m1 or m2 by the introduction of both mutations into the plasmid carrying single mutant *ghoT* alleles. The recovery of the cleavage pattern to that of the wild-type *ghoT* transcript in the double mutant transcript would indicate the importance of RNA secondary structure over sequence recognition in

GhoS cleavage, whereas a reduction in cleavage would indicate that sequence recognition is important. We found that the introduction of both m1 and m2 mutations to restore the stem of the predicted secondary structure (**Fig. 4d**) generated a unique cleavage pattern distinct from that of the native *ghoT* mRNA (**Fig. 4e**). A reduction of the fragments accumulated owing to the m1 mutation along with an increase in large partially cleaved or uncleaved fragments in the mutant transcript with both m1 and m2 mutations compared to the native transcript suggests the importance of sequence recognition during GhoS cleavage. Therefore, GhoS is a specific RNase that limits translation of toxin GhoT by cleaving *ghoT* transcripts.

To provide more evidence of the specificity of the RNase activity of GhoS, we analyzed changes in mRNA levels during production of GhoS compared to the strain with an empty plasmid with a DNA microarray so that we could investigate *in vivo* which of the cell's transcripts may be cleaved by GhoS. Under these conditions, only 20 transcripts had altered mRNA levels, and all were found to be reduced (**Supplementary Table 9**); there were no induced genes. These genes, which were downregulated as a result of GhoS production, were all involved in the biosynthesis and transport of purines and pyrimidines. These results suggest that GhoS selectively cleaves only a few cellular targets.

To further corroborate the findings in the DNA microarray, we performed qRT-PCR with seven genes (*purM*, *purH*, *purE*, *pyrI*, *pyrB*, *carA* and *carB*), with total RNA isolated under the same culture conditions used in the DNA microarray experiment. In each case, the qRT-PCR results showed a decreased RNA abundance upon GhoS production, which matched the microarray results (**Supplementary Table 9**). Although *ghoT* expression was unaltered in the microarray analysis, qRT-PCR performed with duplicate samples on three independent occasions showed that *ghoT* expression was decreased by at least a factor of three upon production of GhoS.

## GhoT increases early biofilm formation

Because toxin-antitoxin systems affect biofilm formation[4,5] and as we identified *mqsR* as one of the highly regulated genes in *E. coli* biofilm cells when compared to planktonic cells[4], we investigated the impact of GhoT-GhoS on biofilm formation. Deletion of *ghoT* decreased biofilm formation at 8 h in LB medium at 30 °C (factor of 4.6) and 37 °C (factor of 4.9), whereas deletion of *ghoS* increased biofilm formation significantly ($P < 0.05$) (up to 6.1-fold) at 30 °C and 37 °C at 8 h (**Supplementary Fig. 10a**). Swimming motility was also slightly reduced when *ghoT* was deleted, whereas
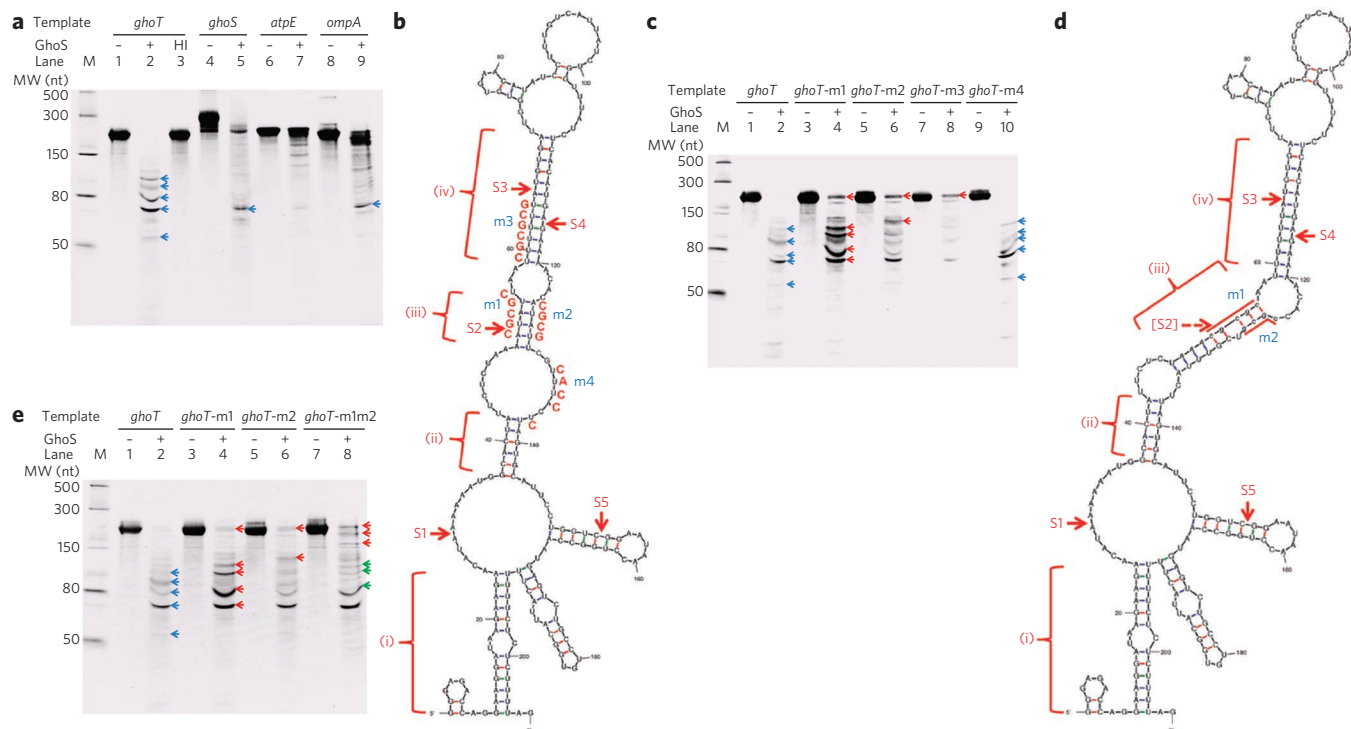
**Figure 4 | GhoS cleavage of native and altered *ghoT* transcripts. (a)** GhoS cleavage reaction with native transcripts of *ghoT* (207 nt), *ghoS* (311 nt), *atpE* (189 nt) and *ompA* (211 nt). HI, heat-inactivated GhoS; MW, low-range single-stranded RNA ladder. The blue arrows indicate the main fragments generated after cleavage. **(b)** Predicted secondary structure of *in vitro* synthesized *ghoT* mRNA. Capital red letters indicate the changed nt for mutations m1, m2, m3 and m4. S1, S2, S3, S4 and S5 indicate the cleavage sites based on RNA sequencing. The four main sections in the structure are indicated with numbers i, ii, iii and iv. The RNA secondary structure was obtained using Mfold software. **(c)** GhoS cleavage reaction with transcripts of *ghoT* (207 nt) with mutations m1, m2, m3 and m4. The red arrows indicate the fragments generated or increased in the mutant transcripts after cleavage. **(d)** Predicted secondary structure of *in vitro* synthesized *ghoT*m1m2 mRNA. The mutated *ghoT*m1m2 cleavage site is indicated by two solid red lines. **(e)** GhoS cleavage reaction with transcripts of *ghoT* (207 nt) with mutations m1, m2 and m1m2 (207 nt). The green arrows indicate the reduced fragments after the introduction of the second mutation. For the reactions shown in **a**, **c** and **e**, 2 μg of *in vitro* synthesized transcripts were incubated with (−) or without (+) 30 μg of purified GhoS at 37 °C for 3 h and analyzed by gel electrophoresis.

the deletion of *ghoS* increased cell motility approximately two-fold (**Supplementary Fig. 10b**). These results show that GhoS and GhoT affect early biofilm formation and swimming motility.

## DISCUSSION

Collectively, our results strongly support that GhoT-GhoS forms a new type V toxin-antitoxin pair. These results are: (i) both proteins are small; (ii) the genes form an operon (*ghoST*) as they are transcribed together and there are only 27 bp between the coding regions of the two genes; (iii) GhoT functions as a presumed membrane toxin that not only stops growth but also, in high concentrations, lyses cells; (iv) GhoS blocks GhoT-mediated toxicity by specifically cleaving *ghoT* transcripts at 5′-UNNU(A/C)N(A/G)(A/U)A(A/U)-3′ sites and preventing its translation; and (v) deletion of antitoxin GhoS in the presence of GhoT is lethal. As a new toxin-antitoxin system, GhoT is to our knowledge the first chromosomal membrane-damaging protein to be neutralized by a protein antitoxin (as compared to the toxin TisB, which damages membranes as a type I toxin-antitoxin system[38]). GhoS is also to our knowledge the first antitoxin to inhibit a toxin by cleaving its mRNA; hence, it creates a new paradigm for toxin-antitoxin systems (we propose the type V designation). Furthermore, the GhoT-GhoS toxin-antitoxin system is unique in that antitoxin GhoS is not proteolytically degraded during stress, and GhoS is unusual in that it does not bind its putative promoter region. For comparison, the antitoxin of the ζ-ε toxin-antitoxin system from plasmid pSM19035 also has no role in transcriptional control, but

instead the toxin-antitoxin operon is repressed by a global regulator ω encoded by a gene within the same operon[39]; however, no such regulator for GhoT-GhoS has been identified. Also, the genomic *mazEF* operon of *Staphylococcus aureus* is not autoregulated by the antitoxin but is instead regulated by an alternative sigma factor encoded by a gene downstream of the *mazEF* operon[40]. These examples illustrate the diversity of toxin-antitoxin systems in terms of function and regulation.

Our central model for the genetic basis of persister cell formation is that toxin-antitoxin pairs have a primary role because toxin activity induces a state of dormancy[41,42]. This, in turn, allows cells to escape the effects of antibiotics. Here we identify a new toxin, GhoT, that increases persistence by damaging the cell membrane. The precise mechanism by which GhoT leads to the loss of membrane integrity while rendering the cells dormant (viable) in the presence of ampicillin is currently unclear but possibly involves proton pumps or interaction with other membrane proteins, among other possibilities. Because MqsR reduces the production of virtually all proteins, including OmpA and OmpF, which results in the enrichment of the small transmembrane protein GhoT, it is possible that MqsR increases persistence through the tight control of outer membrane and inner membrane permeability. Another transmembrane peptide, TisB, has been recently shown to increase persistence by decreasing the proton motive force and amount of ATP in the cell, thus leading to the formation of dormant cells upon antibiotic stress[7]. Similar to production of GhoT, production of TisB also leads to cell death by damaging the inner membrane[38].

Collectively, these findings show that certain transmembrane proteins are stress-response elements that are actively involved in persistence.

GhoT resembles the Hok toxin of type I toxin-antitoxin pair Hok-Sok from plasmid R1 (refs. 43,44). Five other *hok* homologous loci have been identified in the *E. coli* K-12 genome: *hokA*, *hokB*, *hokC*, *hokD* and *hokE*. However, all of them seem to be inactivated by various mutations, including insertion element transposition or point mutations[45]. Hok uses postsegregational killing to stabilize the R1 plasmid[43], but the role of Hok-like toxins as chromosomal loci remains unclear. Also, the link between toxin-antitoxin systems and cell death is controversial[10]. Here, we show that GhoT encodes a putative membrane-damaging protein that, in turn, causes persistence at low doses and cell death at high doses. However, it currently is not clear whether the production of GhoT leads to programmed cell death; that is, perturbing the bacterial membrane by increasing cellular GhoT may be an initial requisite to induce persistence because it causes loss of membrane potential (cell death is not required and may be an artifact of high *ghoT* expression).

Although speculative, our results on this new toxin-antitoxin system have several implications for bacterial cell physiology. The first is that the MqsR-MqsA toxin-antitoxin system may control persistence through differential mRNA decay via the GhoT-GhoS toxin-antitoxin system, which would indicate that toxin-antitoxin systems can regulate one another. If *ghoS* mRNA is preferentially cleaved over *ghoT* by MqsR under MqsR-activating conditions, GhoT translated from the enriched *ghoT* RNA would subsequently lead to the formation of ghost cells as well as higher persistence. This delicate control between the two toxin-antitoxin systems requires additional detailed investigation. Furthermore, the close relationship between GhoS and the CAS2 CRISPR system suggests that this type of specific RNA cleavage is a general and powerful post-transcriptional approach that has evolved for several purposes in the cell, from controlling cell growth to preventing phage attack. There are suggestions that such systems are global. A report of a similar endoRNase VapD from *Helicobacter pylori*[46], also found in a two-gene operon and also related to CAS2 protein SSO1404, concluded that the RNase was not an antitoxin. However, reinterpreting those data in light of our results suggests that it might be a more parsimonious explanation for the RNase to be the antitoxin, suggesting that similar type V toxin-antitoxin systems may be found elsewhere. As a result, toxin-antitoxin systems are even more complex and diverse in their regulator roles.

## METHODS

**Persister cell formation assay.** Persister cell measurements were performed as described[6] with slight modifications. To determine the number of persister cells in the presence of MqsR, we introduced pCA24N-*mqsR* into 14 isogenic single-gene knockouts (**Supplementary Table 2**). Overnight cultures of these cells were inoculated into LB medium with chloramphenicol at an initial turbidity at 600 nm of 0.05 and were grown for 2.5 h. To induce *mqsR*, we added 1 mM IPTG for 2 h. Cells were washed with 0.85% (w/v) NaCl, and the turbidity was adjusted to 1. After exposure to 100 µg ml⁻¹ ampicillin for 2 h, cells were serially diluted in 0.85% (w/v) NaCl solution and applied as 10-µl drops to LB plates with chloramphenicol to determine persister cell number[47]. To further evaluate the effect of removing *ghoT* on the formation of persister cells via MqsR, we extended the exposure of 100 µg ml⁻¹ ampicillin to up to 6 h for BW25113/pCA24N, BW25113/pCA24N-*mqsR* and Δ*ghoT*/pCA24N-*mqsR* and for Δ*ghoT*/pCA24N-*ghoT* and Δ*ghoT*/pCA24N. Three independent cultures were used.

**Toxicity assay.** Overnight cultures of strains producing GhoT via pCA24N-*ghoT*, GhoS via pBS(Kan)-*ghoS* and variant GhoSX (truncated GhoS with a stop codon introduced at Tyr16) via pBS(Kan)-*ghoS*X were inoculated into 25 ml of LB medium with kanamycin and chloramphenicol (to maintain both plasmids) to an initial turbidity at 600 nm of ~0.1 with 0.5 mM IPTG, and the turbidity was recorded to determine growth. Three independent cultures were used.

**Microscopy.** To observe ghost cells, we diluted overnight cultures of BW25113/pCA24N-*ghoT*/pBS(Kan) and BW25113/pCA24N-*ghoT*/pBS(Kan)-*ghoS* to a turbidity of 0.05 at 600 nm and grew them to a turbidity of 0.1, and then 0.5 mM IPTG was added to induce *ghoT* and *ghoS*. Cells were collected after 8 h,

washed and resuspended in 0.85% (w/v) NaCl. Cells were then visualized with light microscopy (Zeiss Axiophot) using an oil immersion objective (63×).

**RT-PCR and qRT-PCR.** To determine whether *ghoS* and *ghoT* are cotranscribed, we performed RT-PCR[15]. Total RNA was isolated[4] from BW25113 grown at 37 °C during the exponential phase (turbidity was 0.5) with RNAlater (Applied Biosystems). cDNA was synthesized from total RNA with reverse transcriptase (Promega) and random hexamer primers (Invitrogen)[4]. Standard PCR was performed with Pfu DNA polymerase using 50 ng of cDNA as template and with primer pair *ghoS*-f and *ghoT*-r and primer pair *ghoS*-f and *ghoS*-r (**Supplementary Table 3**). Total RNA and genomic DNA (~50 ng) were also used as templates for negative and positive controls, respectively.

For qRT-PCR, 50 ng of total RNA was used in each reaction using the Power SYBR Green RNA-to-C$_T$ 1-Step Kit and the StepOne Real-Time PCR System (Applied Biosystems). Primers were annealed at 60 °C, and *rrsG*[9] expression was used to normalize the data.

**Site-directed mutagenesis.** Site-directed mutagenesis[9] was used to introduce a stop codon into the coding region of *ghoS* in pBS(Kan)-*ghoS* using primer pair GhoS-X-f and GhoS-X-r (**Supplementary Table 3**). DNA sequencing using the BigDye Terminator Cycle Sequencing kit was performed to confirm the targeted mutations at these sites.

**Crystal violet biofilm assay.** Biofilm formation was assayed in 96-well polystyrene plates using 0.1% (w/v) crystal violet staining[48]. Briefly, overnight cultures of the wild-type, Δ*ghoS* and Δ*ghoT* strains were inoculated at an initial turbidity at 600 nm of 0.05 and grown without shaking for 8 h and 24 h in LB medium. Biofilm formation was normalized by the bacterial growth for each strain (turbidity at 620 nm), and two independent cultures were used for each strain.

**Swimming motility assay.** Cell motility was examined as described previously on low-salt soft agar plates (1% (w/v) tryptone, 0.25% (w/v) NaCl and 0.3% (w/v) agar), in which the wild-type BW25113 is motile[49].

**GhoS RNA cleavage assay.** For the synthesis of *ghoS*, *ghoT*, *atpE*, *ompA* and *ghoT* mRNAs carrying different mutations, PCR products were obtained using the primers shown in **Supplementary Table 7** and were used as templates for *in vitro* transcription with T7 RNA polymerase. The T7 RNA polymerase promoter sequence was included in the forward primers. The primers (without the T7 RNA polymerase promoter sequences) for making the *ghoS* and *ghoT* mRNAs are shown in **Supplementary Figure 1c**. PCR products were gel purified, and 0.5–1 µg of the PCR product was used as the template for the *in vitro* RNA reaction with the AmpliScribe T7-Flash transcription kit (Epicentre). The reaction mixture for the GhoS endoRNase cleavage assay (10 µl) contained 2 µg RNA, 50 mM Tris-HCl (pH 8.5), 100 mM KCl, 2.5 mM MgCl₂ and 30 µg of purified GhoS protein. RNA substrates included *ghoS*, *ghoT*, *atpE*, *ompA*, *ghoT*m1, *ghoT*m2, *ghoT*m3, *ghoT*m4 and *ghoT*m1m2 mRNAs, total RNAs isolated from BW25113 wild-type cells (turbidity ~2.0) and *E. coli* total tRNAs (Roche). The reaction mixture was incubated at 37 °C for 3 h and quenched by the addition of an equal volume of 2× Tris-borate-EDTA (TBE)-urea sample buffer (Invitrogen). To inactivate GhoS, we heated protein samples at 95 °C for 1 h and cooled them before adding to the reactions. The reaction products were resolved by 15% (w/v) TBE-urea gels (Invitrogen).

**Statistical analysis.** Data are presented as means ± s.e.m. of three or more independent cultures. Statistical significance was assessed using two-tailed unpaired Student's *t*-test.

**Additional methods.** Bacterial strains, plasmids and growth conditions; expression and purification of GhoS for NMR studies; construction of GhoS variants; CD; purification of His₆-GhoS for EMSA assays; the EMSA assays; conditions for western blotting; NMR spectroscopy; chemical shift assignments and structure calculation; RNA isolation and whole-transcriptome studies; RNA sequencing; mutagenesis of *ghoT* mRNA; and the persister revival assay are described in the **Supplementary Methods**. Antibiotic concentrations, unless specified otherwise, were 50 µg ml⁻¹ for kanamycin and 30 µg ml⁻¹ or 34 µg ml⁻¹ for chloramphenicol.

## References

1. Gerdes, K., Christensen, S.K. & Lobner-Olesen, A. Prokaryotic toxin-antitoxin stress response loci. *Nat. Rev. Microbiol.* **3**, 371–382 (2005).
2. Hayes, F. & Van Melderen, L. Toxins-antitoxins: diversity, evolution and function. *Crit. Rev. Biochem. Mol. Biol.* **46**, 386–408 (2011).

3. Masuda, H., Tan, Q., Awano, N., Wu, K.-P. & Inouye, M. YeeU enhances the bundling of cytoskeletal polymers of MreB and FtsZ, antagonizing the CbtA (YeeV) toxicity in *Escherichia coli*. *Mol. Microbiol.* **84**, 979–989 (2012).

4. Ren, D., Bedzyk, L.A., Thomas, S.M., Ye, R.W. & Wood, T.K. Gene expression in *Escherichia coli* biofilms. *Appl. Microbiol. Biotechnol.* **64**, 515–524 (2004).

5. Kim, Y., Wang, X., Qun, M., Zhang, X.-S. & Wood, T.K. Toxin-antitoxin systems in *Escherichia coli* influence biofilm formation through YjgK (TabA) and fimbriae. *J. Bacteriol.* **191**, 1258–1267 (2009).

6. Kim, Y. & Wood, T.K. Toxins Hha and CspD and small RNA regulator Hfq are involved in persister cell formation through MqsR in *Escherichia coli*. *Biochem. Biophys. Res. Commun.* **391**, 209–213 (2010).

7. Dörr, T., Vulić, M. & Lewis, K. Ciprofloxacin causes persister formation by inducing the TisB toxin in *Escherichia coli*. *PLoS Biol.* **8**, e1000317 (2010).

8. Hu, Y., Benedik, M.J. & Wood, T.K. Antitoxin DinJ influences the general stress response through transcript stabilizer CspE. *Environ. Microbiol.* **14**, 669–679 (2012).

9. Wang, X. *et al.* Antitoxin MqsA helps mediate the bacterial general stress response. *Nat. Chem. Biol.* **7**, 359–366 (2011).

10. Wang, X. & Wood, T.K. Toxin/antitoxin systems influence biofilm and persister cell formation and the general stress response. *Appl. Environ. Microbiol.* **77**, 5577–5583 (2011).

11. Amitai, S., Kolodkin-Gal, I., Hananya-Meltabashi, M., Sacher, A. & Engelberg-Kulka, H. *Escherichia coli* MazF leads to the simultaneous selective synthesis of both "death proteins" and "survival proteins". *PLoS Genet.* **5**, e1000390 (2009).

12. Belitsky, M. *et al.* The *Escherichia coli* extracellular death factor EDF induces the endoribonucleolytic activities of the toxins MazF and ChpBK. *Mol. Cell* **41**, 625–635 (2011).

13. González Barrios, A.F. *et al.* Autoinducer 2 controls biofilm formation in *Escherichia coli* through a novel motility quorum-sensing regulator (MqsR, B3022). *J. Bacteriol.* **188**, 305–316 (2006).

14. Kim, Y. *et al. Escherichia coli* toxin/antitoxin pair MqsR/MqsA regulate toxin CspD. *Environ. Microbiol.* **12**, 1105–1121 (2010).

15. Yamaguchi, Y., Park, J.-H. & Inouye, M. MqsR, a crucial regulator for quorum sensing and biofilm formation, is a GCU-specific mRNA interferase in *Escherichia coli*. *J. Biol. Chem.* **284**, 28746–28753 (2009).

16. Christensen-Dalsgaard, M., Jørgensen, M.G. & Gerdes, K. Three new RelE-homologous mRNA interferases of *Escherichia coli* differentially induced by environmental stresses. *Mol. Microbiol.* **75**, 333–348 (2010).

17. Domka, J., Lee, J., Bansal, T. & Wood, T.K. Temporal gene-expression in *Escherichia coli* K-12 biofilms. *Environ. Microbiol.* **9**, 332–346 (2007).

18. Lewis, K. Persister cells, dormancy and infectious disease. *Nat. Rev. Microbiol.* **5**, 48–56 (2007).

19. Lewis, K. Persister cells. *Annu. Rev. Microbiol.* **64**, 357–372 (2010).

20. Brown, B.L. *et al.* Three dimensional structure of the MqsR:MqsA complex: a novel TA pair comprised of a toxin homologous to RelE and an antitoxin with unique properties. *PLoS Pathog.* **5**, e1000706 (2009).

21. Keren, I., Shah, D., Spoering, A., Kaldalu, N. & Lewis, K. Specialized persister cells and the mechanism of multidrug tolerance in *Escherichia coli*. *J. Bacteriol.* **186**, 8172–8180 (2004).

22. Correia, F.F. *et al.* Kinase activity of overexpressed HipA is required for growth arrest and multidrug tolerance in *Escherichia coli*. *J. Bacteriol.* **188**, 8360–8367 (2006).

23. Shah, D. *et al.* Persisters: a distinct physiological state of *E. coli*. *BMC Microbiol.* **6**, 53 (2006).

24. Balaban, N.Q., Merrin, J., Chait, R., Kowalik, L. & Leibler, S. Bacterial persistence as a phenotypic switch. *Science* **305**, 1622–1625 (2004).

25. Hofmann, K. & Stoffel, W. TMBASE—a database of membrane spanning protein segments. *Biol. Chem. Hoppe-Seyler* **374**, 166 (1993).

26. Faridani, O.R., Nikravesh, A., Pandey, D.P., Gerdes, K. & Good, L. Competitive inhibition of natural antisense Sok-RNA interactions activates Hok-mediated cell killing in *Escherichia coli*. *Nucleic Acids Res.* **34**, 5915–5922 (2006).

27. Baba, T. *et al.* Construction of *Escherichia coli* K-12 in-frame, single-gene knockout mutants: the Keio collection. *Mol. Syst. Biol.* **2**, 2006.0008 (2006).

28. Van Melderen, L. & Saavedra De Bast, M. Bacterial toxin–antitoxin systems: more than selfish entities? *PLoS Genet.* **5**, e1000437 (2009).

29. Güntert, P. Automated NMR structure calculation with CYANA. *Methods Mol. Biol.* **278**, 353–378 (2004).

30. Herrmann, T., Guntert, P. & Wuthrich, K. Protein NMR structure determination with automated NOE-identification in the NOESY spectra using the new software ATNOS. *J. Biomol. NMR* **24**, 171–189 (2002).

31. Herrmann, T., Guntert, P. & Wuthrich, K. Protein NMR structure determination with automated NOE assignment using the new software CANDID and the torsion angle dynamics algorithm DYANA. *J. Mol. Biol.* **319**, 209–227 (2002).

32. Brünger, A.T. *et al.* Crystallography & NMR system: a new software suite for macromolecular structure determination. *Acta Crystallogr. D Biol. Crystallogr.* **54**, 905–921 (1998).

33. Holm, L., Kaariainen, S., Rosenstrom, P. & Schenkel, A. Searching protein structure databases with DaliLite v.3. *Bioinformatics* **24**, 2780–2781 (2008).

34. Orengo, C.A., Jones, D.T. & Thornton, J.M. Protein superfamilies and domain superfolds. *Nature* **372**, 631–634 (1994).

35. Beloglazova, N. *et al.* A novel family of sequence-specific endoribonucleases associated with the clustered regularly interspaced short palindromic repeats. *J. Biol. Chem.* **283**, 20361–20371 (2008).

36. Samai, P., Smith, P. & Shuman, S. Structure of a CRISPR-associated protein Cas2 from *Desulfovibrio vulgaris*. *Acta Crystallogr. Sect. F Struct. Biol. Cryst. Commun.* **66**, 1552–1556 (2010).

37. Beloglazova, N. *et al.* A novel family of sequence-specific endoribonucleases associated with the clustered regularly interspaced short palindromic repeats. *J. Biol. Chem.* **283**, 20361–20371 (2008).

38. Unoson, C. & Wagner, E.G.H. A small SOS-induced toxin is targeted against the inner membrane in *Escherichia coli*. *Mol. Microbiol.* **70**, 258–270 (2008).

39. de la Hoz, A.B. *et al.* Plasmid copy-number control and better-than-random segregation genes of pSM19035 share a common regulator. *Proc. Natl. Acad. Sci. USA* **97**, 728–733 (2000).

40. Donegan, N.P. & Cheung, A.L. Regulation of the *mazEF* toxin-antitoxin module in *Staphylococcus aureus* and its impact on *sigB* expression. *J. Bacteriol.* **191**, 2795–2805 (2009).

41. Jayaraman, R. Bacterial persistence: some new insights into an old phenomenon. *J. Biosci.* **33**, 795–805 (2008).

42. Maisonneuve, E., Shakespeare, L.J., Jørgensen, M.G. & Gerdes, K. Bacterial persistence by RNA endonucleases. *Proc. Natl. Acad. Sci. USA* **108**, 13206–13211 (2011).

43. Gerdes, K. The *parB* (*hok/sok*) locus of plasmid R1: a general purpose plasmid stabilization system. *Nat. Biotechnol.* **6**, 1402–1405 (1988).

44. Pecota, D.C. & Wood, T.K. Exclusion of T4 phage by the *hok/sok* killer locus from plasmid R1. *J. Bacteriol.* **178**, 2044–2050 (1996).

45. Pedersen, K. & Gerdes, K. Multiple *hok* genes on the chromosome of *Escherichia coli*. *Mol. Microbiol.* **32**, 1090–1102 (1999).

46. Kwon, A.-R *et al.* Structural and biochemical characterization of HP0315 from *Helicobacter pylori* as a VapD protein with an endoribonuclease activity. *Nucleic Acids Res.* **40**, 4216–4228 (2012).

47. Donegan, K., Matyac, C., Seidler, R. & Porteous, A. Evaluation of methods for sampling, recovery, and enumeration of bacteria applied to the phylloplane. *Appl. Environ. Microbiol.* **57**, 51–56 (1991).

48. Fletcher, M. The effects of culture concentration and age, time, and temperature on bacterial attachment to polystyrene. *Can. J. Microbiol.* **23**, 1–6 (1977).

49. Barrios, A.F., Zuo, R., Ren, D. & Wood, T.K. Hha, YbaJ, and OmpA regulate *Escherichia coli* K12 biofilm formation and conjugation plasmids abolish motility. *Biotechnol. Bioeng.* **93**, 188–200 (2006).

## Acknowledgments

## Author contributions

T.K.W., X.W., R.P., W.P. and M.J.B. designed the experiments. X.W., H.-Y.C., D.M.L., S.H.H., D.O.O., V.S.-T. and C.Q. performed the *in vivo* and *in vitro* assays for the functional studies of GhoT and GhoS and for the regulation of the *ghoST* operon. K.Z. and D.M.L. purified GhoS, and D.M.L. and W.P. completed the NMR structure with help from T.H. with the structure calculations and refinement. T.K.W. and X.W. authored the nonstructural parts of the manuscript, and R.P. and W.P. wrote the structural sections. All authors discussed the results and commented on the manuscript.

## Competing financial interests

The authors declare no competing financial interests.

## Additional information

Supplementary information is available in the online version of the paper. Reprints and permissions information is available online at http://www.nature.com/reprints/index.html. Correspondence and requests for materials should be addressed to T.K.W. or R.P.